Corrosion behavior of experimental nickel-bearing carbon steels evaluated using field and electrochemical tests

http://dx.doi.org/10.1590/0370-44672016710173

Vanessa Lins[1]
Edelize Angelica Gomes[2]
Cíntia Gonçalves Costa[3]
Maria das Mercês Reis Castro[4]
Rogerio Augusto Carneiro[5]

[1]Universidade Federal de Minas Gerais – UFMG, Escola de Engenharia, Departamento de Química, Belo Horizonte - Minas Gerais – Brasil.
vlins@deq.ufmg.br

[2]Universidade Federal de Minas Gerais – UFMG, Escola de Engenharia, Departamento de Química, Belo Horizonte - Minas Gerais – Brasil.
edelizeg@hotmail.com

[3]Universidade Federal de Minas Gerais – UFMG, Escola de Engenharia, Departamento de Química, Belo Horizonte - Minas Gerais – Brasil.
cintiagf@gmail.com

[4]Universidade Federal de Minas Gerais – UFMG, Escola de Engenharia, Departamento de Química, Belo Horizonte - Minas Gerais – Brasil.
deia@deq.ufmg.br

[5]USIMINAS – Usinas Siderúrgicas de Minas Gerais, Belo Horizonte - Minas Gerais – Brasil.
rogerio.carneiro@usiminas.com

Abstract

The aim of this study was to evaluate the corrosion resistance of Ni-bearing carbon steels used in outdoor structures from short-term experimental techniques and compare with the long-term field test data. The carbon steels studied were two experimental steels, produced in a pilot plant, and alloyed with nickel, copper, silicon and molybdenum (Ni-Cu-Si and Ni-Cu-Mo-Si steels), one carbon steel and one commercial Cr-Cu-Si alloyed steel. The atmospheric corrosion resistance of low alloyed carbon steels was evaluated by using field tests for eight years in a marine station, and their electrochemical behavior was studied in laboratory using the electrochemical impedance spectroscopy in aqueous electrolytes containing chlorides. The Ni-Cu-Si and Ni-Cu-Mo-Si steels showed the lowest corrosion rates which decreased as the time increased after eight years of exposure in marine atmosphere. The classification of the low alloyed steels considering the corrosion resistance using electrochemical tests in 10% m/v NaCl solution was similar to rating using field tests in a marine station.

Keywords: Ni-bearing carbon steel; field test; atmospheric corrosion; electrochemical impedance spectroscopy.

1. Introduction

Low alloyed steels are used in the automotive, home appliances and civil construction industries. However, the conventional low alloyed carbon steels are not resistant in marine atmospheres (Morcillo *et al*., 2014). There are many steel structures in coastal areas. Thus it is necessary to use high resistant steels against the marine atmospheric corrosion (Nishimura, 2007, Itou *et al*., 2000). Ni-bearing weathering steels have increased resistance against corrosion (Kimura ., 2004), which varies almost linearly with increasing the content of the alloying element in the steel. Good corrosion resistance of the Ni advanced weathering steel can be attributed to fine grain-size distributions of the inner layers and the formation of $Fe_{3-x}NixO_4$ (Kimura *et al*., 2004). In conventional weathering steels, the rust (FeOOH) becomes positively charged by attached H^+ ions produced by hydrolysis of iron ions or iron chlorides. However, the inner rust of advanced weathering steel contains $Fe_{3-x}NixO_4$, which is negatively charged. The rust repels chloride ions from rust/steel interface (Kimura *et al*., 2004).

Copper, chromium and phosphorous are preferably concentrated in the inner regions of the oxide layers, while the outer rust layer is chromium-depleted (Wang *et al*., 2013). Copper is located on the crack surface of the inner layer, where the sulfur from atmosphere compounds is also observed at a higher intensity (Yamashita *et al*., 1994; Yamashita and Misawa, 2000; Shiotani *et al*., 2000). When copper reacts with these sulfur compounds to form insoluble CuS, copper reduces the generation of SO_4^{2-} ions which form soluble compounds with iron, which are easily removed. Thus, copper favors the corrosion resistance. Copper also retards the crystal growth of an oxide layer, promoting structure refinement, decreasing conductivity of the oxide layer, adsorbing on the steel surface, and accelerating the uniform dissolution of the steel (Zhang *et al*., 2002; Wang *et al*., 2013), which contributes to the formation of the oxide layer in the initial stages of the corrosion process (Wang *et al*., 2013).

It is well known that cyclic accelerated corrosion tests are adequate for studying the atmospheric corrosion resistance of metals in a shorter time than field tests, maintaining a similar mechanism. However, the complexity of the effect of the variables that operate in the atmosphere, the synergy between them, and the particularity of the kinetic atmospheric processes are conducive for performing field testing for a consistent study of atmospheric corrosion resistance.

The viability to predict the corrosion behavior of low alloyed carbon steels using accelerated electrochemical tests in saline solutions containing 3.5%wt. and 10%wt was studied. The classification of the low alloyed steels considering the corrosion resistance using electrochemical tests in a saline solution was compared to ratings using field tests in a marine station.

The carbon steels studied were two experimental steels, produced in a pilot plant, and alloyed with nickel, copper, silicon and molybdenum (Ni-Cu-Si and Ni-Cu-Mo-Si samples named), one carbon steel and one commercial Cr-Cu-Si alloyed steel.

2. Material and methods

The carbon steels studied were two experimental steels, produced in a pilot plant, and alloyed with nickel, copper, silicon and molybdenum (Ni-Cu-Si and Ni-Cu-Mo-Si steels), whose corrosion resistance was compared with two commercial steels: one carbon steel and one conventional Cr-Cu-Si alloyed steel.

The carbon contents of the steel were analyzed using the combustion technique with detection by infrared, by using the LECO 444 LS equipment, Leco Corporation. Molybdenum, nickel, chromium, and copper concentrations were evaluated by using inductively coupled plasma optical emission spectrometry, ICP-OES, Spectroflame Modula of the Spectra. Manganese, silicon and phosphorus were analyzed by using the SRS 3000 Sequential X-Ray Spectrometer, Siemens.

Metallographic analysis was performed using the chemical attack with 4mL HNO_3 and 96 mL of ethyl alcohol, optical and scanning electron microscopy by using Jeol Model 6360 LV equipment.

2.1 Field tests

The complexity of the effect of the variables that operate in the atmosphere, the synergy between them, and the particularity of the kinetic atmospheric processes are conducive for performing field testing for a consistent study of atmospheric corrosion resistance. The corrosion resistance of the steels was analyzed by a field test in a marine atmosphere for eight years according to the ISO 9226:2012 Standard. In a corrosion station, the specimens were fixed with an inclination of 30° from the horizontal and the exposed surface oriented toward the north. At the beginning, sixteen samples were exposed for each steel studied. Two samples were removed every 12 months to be weighed and characterized. The standard deviation was of 5%.

Before testing, all specimens were cleaned with abrasives to near white metal (Sa 2 ½) and residual grit were cleaned with a jet of clean, dry air and the soft brush. The samples were weighed with an accuracy of 1 mg using an analytical balance Sartorius CC 3000, and the dimensions and total area were measured.

The station was located in Rio de Janeiro State, 48.7 m above sea level, at 23°00'49 "S latitude and 42°00'56 "W longitude. The marine station showed an average chloride deposition rate of 102 mg Cl^-/m^2, determined by the method of wet candle, and corrosiveness of 0.6 kgFe/m^2year (Alvarenga *et al*., 2006), so that it can be classified as highly aggressive (C4) in accordance with ISO 9223.

After the atmospheric corrosion test, the samples were mechanically cleaned to remove non-adherent corrosion products, using brush and scraping their surfaces. For cleaning the adherent oxide layer, a hydrochloric acid solution was used (concentration 1:1) with a hexamethylenetetramine organic inhibitor (concentration 3.5 g/L). The samples were washed and brushed in water, immersed in the solvent acetone and dried with clean air and then immediately weighed.

The oxides formed on the steel samples exposed at marine atmosphere for eight years were analyzed using an X-ray diffractometer, PHILIPS, model PW 1710, equipped with Cu tube, CuKα radiation and graphite monochromator crystal.

2.2 Electrochemical tests

The samples were blasted using steel shot, on both sides of the plate. After blasting, the samples were cut into samples of 1 cm^2 in area, washed with acetone and dried with hot air. Samples were polished with sandpapers of 180, 320, 600, 1200 and 1500 mesh and polished with alumina paste and then washed with ethanol. Before EIS analysis, the steel samples were immersed in a 10% m/v NaCl aqueous solution for one hour to measure the open circuit potential. The electrochemical impedance spectroscopy was performed using an IVIUM potentiostat, potential amplitude of 10 mV (in relation to the corrosion potential), frequency range of 100 kHz to 0.01 Hz. The reference electrode used was Ag/AgCl and platinum was the counter electrode. The electrolyte used was aqueous solutions of NaCl (3.5% m/v and 10% m/v). The electrochemical measurements were performed in quintuplicate. The data of electrochemical impedance spectroscopy were analyzed by ZSimpWin software, using a correspondent electrical circuit.

3. Results and discussion

The chemical composition of steels studied is shown in Table 1.

Steel	C	Mn	P	S	Ni	Cu	Mo	Si	Cr	Al
Ni-Cu-Si	0.10	0.70	0.015	0.01	2.0	0.080	-	0.20	-	0.03
Ni-Cu-Mo-Si	0.10	0.70	0.015	0.01	2.0	0.080	0.40	1.10	-	0.03
Cr-Cu-Si	0.08	0.55	0.032	0.005	0.014	0.090	-	1.20	0.220	0.04
SAE 1006	0.06	0.47	0.017	0.006	0.018	0.012	-	0.20	0.025	0.03

Table 1
Chemical composition of steels (wt.%).

Additions of Ni in the experimental steels are of 2 wt.%. Additions of copper in low alloyed steels are of 0.080 wt.% in the experimental steels and of 0.090 wt.% in Cr-Cu-Si carbon steels. Additions of silicon are of 1.10 wt.% in Ni-Cu-Mo-Si steels, of 0.20 wt.% in Ni-Cu-Si and 1.20 wt.% in Cr-Cu-Si steels. Molybdenum content in Ni-Cu-Mo-Si is of 0.40 wt.%.

Figure 1 shows the bainite microstructure of Ni-Cu-Mo-Si carbon steel. The Ni-Cu-Si, Cr-Cu-Si and the carbon steel presented a ferrite/perlite microstructure.

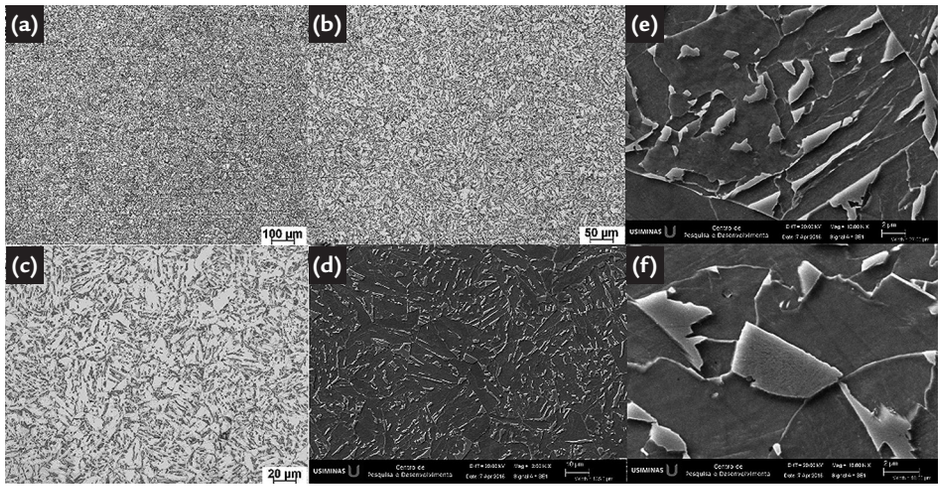

Figure 1
Micrographs of Ni-Cu-Mo-Si carbon steel with different magnifications with bar sizes of: a) 100 µm, b) 50 µm, c) 20 µm, d) 10 µm, e) 7 µm and f) 2 µm.

3.1 Field testing

The Ni-Cu-Si and Ni-Cu-Mo-Si steels showed lower corrosion rates, which decreased as the time increased (Fig.2).

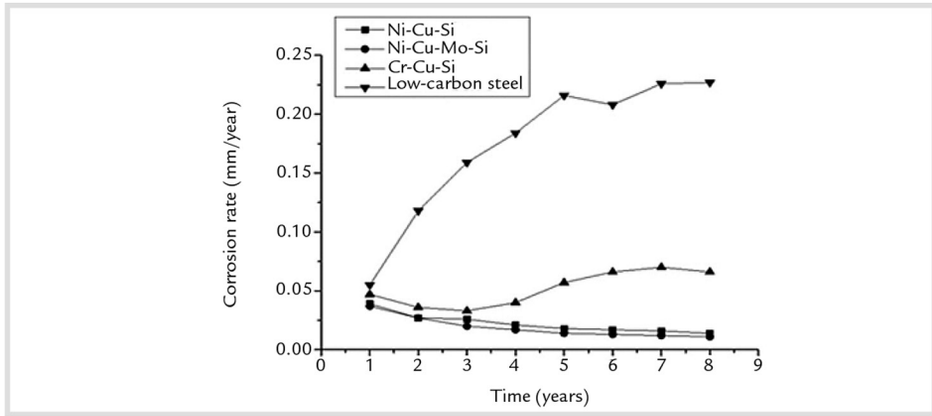

Figure 2
Corrosion rate of steels after eight years of exposure in marine atmosphere.

Application of weathering steels in coastal regions requires high marine atmospheric corrosion-resistant steels. Thus this utilization promoted the development of the Ni-bearing steels with up to 3wt.% Ni (Takemura *et al*., 2000; Kimura *et al*., 2004). The fine grain-size distributions of the inner layers and the formation of $Fe_{3-x}NixO_4$ (Kimura *et al*., 2004) confer on Ni-bearing steels superior atmospheric corrosion resistance as shown in Fig. 2. In conventional weathering steels, the rust (FeOOH) becomes positively charged by attached H^+ ions produced by hydrolysis of iron ions or iron chlorides. However, the inner rust of advanced weathering steel containing $Fe_{3-x}NixO_4$ is negatively charged and repels chloride ions from rust/steel interface (Kimura *et al*., 2004). The Ni-substituted oxides are very stable even in presence of aggressive ions such as chloride ions present in marine atmospheres. The stability and cationic selectivity of Ni–substituted oxides that form the inner layer act as a barrier and prevent water and corrosive ions reach the steel substrate, providing great performance against corrosion in environments rich in chloride ions.

Silicon was added in the Ni-Cu-Mo-Si steels and in the Cr-Cu-Si. Silicon has a beneficial effect on the resistance to atmospheric corrosion of steels (Nishimura,

2007; Toshiyasu, 2007). This element promotes the formation of an internal nano-sized oxide layer enriched in Si, compact and adherent. In addition to the function as a physical barrier, hindering the access of water and corrosive agents to the steel substrate, this Si- substituted layer, similar to that Ni- substituted and Cr-substituted oxide layer, has cationic permeability and prevents that corrosive anions such as chlorides reach the substrate (Nishimura, 2007; Toshiyasu, 2007). The addition of silicon in Fe alloys enhances the protection and densification of rust layers in Si-bearing steels, increasing its atmospheric corrosion resistance (Chen *et al*., 2005).

The carbon steel showed the lowest atmospheric corrosion resistance as expected and was used for comparison. The corrosion rate of low carbon steel increased almost linearly for five years and then tended to stabilize.

The atmospheric corrosion rate of the Cr-Cu-Si decreased as the time increased in the initial three years, then increased and stabilized after six years. After eight years of exposure in marine atmosphere, the Cr-Cu-Si and carbon steels showed a lower corrosion resistance than the Ni-bearing steels as shown in Figure 2.

The beneficial effect of copper operates in the Cr-Cu-Si, but also in the Ni-Cu-Si and Ni-Cu-Mo-Si steels which showed the highest corrosion resistance in the marine atmosphere.

The weathering steel (Cr-Cu-Si) showed the addition of phosphorous and chromium which is beneficial in relation to the atmospheric corrosion resistance (Kihira *et al*., 1990; Chen *et al*., 2005). The addition of phosphorous to the weathering steel enriched the oxide layer with phosphate compounds (Kihira *et al*., 1990). It is also suggested that the bi-acid phosphate ion (H_2PO_{4-}) accelerates the formation of the protective layer and reduces the crystal growth of oxides, contributing to its refinement (Kihira *et al*., 1990).

Chromium, in turn, partially replaces iron in the crystal structure of goethite, mainly found in the innermost part of the oxide layer, as in the other phases that predominate in the outer part (Wang *et al*., 2013). The nanophase Cr^- substituted goethite has a cationic selectivity, hindering the passage of anions (Wang *et al*., 2013). Thus, the inner layer acts as a barrier and prevents water and corrosive anions reach the interface with the steel substrate. However, although providing high protection in rural, urban and industrial atmospheres, this layer is not efficient when chloride ions are present, given that such ions can cross the corrosion product layer and cause accelerated corrosion of the steel substrate (Kage *et al*., 2005). Chromium does not occupy a specific site in the crystal structure, which makes the structure unstable around its atom. These chromium atoms are located on the surfaces or in the grain boundaries of the particles of the constituents of the oxide layer, so that it is more likely that they interact with ions from the atmosphere and, depending on the amount and aggressiveness these ions, the oxide layer loses its protective capability (Kage *et al*,. 2005). In this work, the atmospheric corrosion resistance of the Cr-Cu-Si steel was lower than the Ni-bearing steels.

X-ray diffraction analysis identified the crystalline phases of oxides (Figure 3). Magnetite was the main compound identified in the oxide layer on the Cr-Cu-Si and carbon steels. Goethite (α –FeOOH) and lepidocrocite (γ-FeOOH) were the phases in higher concentration in the oxide layer of the Ni-Cu-Si and the Ni-Cu-Si-Mo steels. The goethite formed on the surface of Ni-Cu-Si and Ni-Cu-Si-Mo steels probably was Ni-substituted, and Si-substituted and was present in the inner layer as discussed.

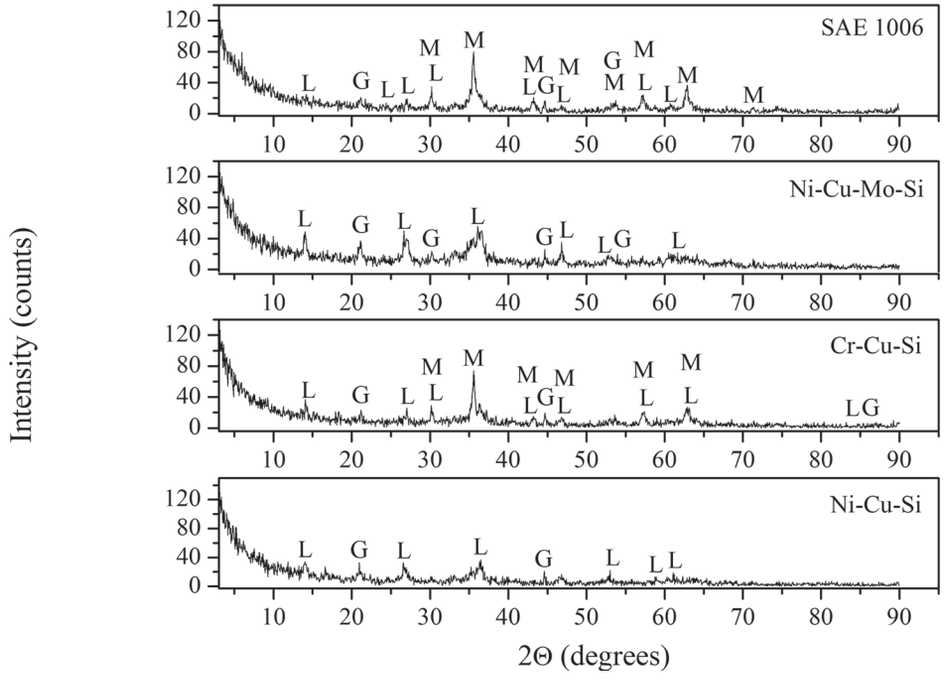

Figure 3
X-ray diffraction analysis of oxides formed on surfaces of SAE 1006, Ni-Cu-Mo-Si, Cr-Cu-Si and Ni-Cu-Si after 8 years of exposure in marine atmosphere. The phases identified were magnetite (M), goethite (G) and lepidocrocite (L).

Literature reports that differences in the relative amounts of oxides, crystal size and oxide structure vary according to the kind of atmosphere to which the steel is exposed (Yamashita *et al*., 2001). Most of the goethite (α-FeOOH) formed in the inner layer of the oxides of mild steel has a crystal diameter up to 100 nm, whereas in weathering steels such diameter is below 10 nm (Yamashita *et al*., 2001). The crystals of lepidocrocite (γ-FeOOH) of the outer oxide layer of carbon steels are also much larger than the nanoparticles of goethite on the weathering steels (Yamashita *et al*., 2001). While weathering steels have an inner layer of oxides rich in goethite ultrathin, Cr-substituted and Si-substituted, compact and corrosion resistant, mild steels feature a mixture of coarse particles of lepidocrocite and

goethite containing voids and cracks which reduce their resistance against corrosion (Yamashita *et al*., 2001). Some researchers have drawn conclusions about the mechanism of corrosion from the composition of the oxides. For example, some studies indicate that the lepidocrocite (γ-FeOOH) forms first and then is converted into α-FeOOH and Fe_3O_4 (Chen *et al*., 2005).

Rust becomes rich in Fe_3O_4, but poor in γ-FeOOH in coastal regions, while the rust formed in rural areas is rich in α-FeOOH phase (Wang *et al*., 2013), which is stable, compact and dense. Therefore, the presence of that phase in high quantity in the oxide layer is useful for improving the corrosion resistance of the steel. The α-FeOOH phase was confirmed in the samples of the steels studied in this research. After 5 years of exposure, Wang *et al.* (2013) observed that the corrosion rates in all steels decreased with increasing exposure time. Therefore, a larger amount of α-FeOOH phase on the surface of weathering steels favors the reduction of the corrosion rate after exposure to the outdoors. Moreover, β-FeOOH phase was not found in the rust layer, this fact was attributed to the Cl^-concentration in the atmosphere which is below the critical value (Wang *et al*., 2013). The absence of β-FeOOH phase on the surface of the commercial weathering steel (Cr-Cu-Si) studied herein has also been proven by the test of X-ray diffraction. Ma *et al.* (2009) studied the effect of Cl^-ions in the atmospheric corrosion rate of carbon steel. The results showed that, under the condition of deposition of large amounts of chloride, the presence of Cl^- is conducive to the formation of β-FeOOH phase. At low concentrations of chlorides, the transformation of γ-FeOOH to α-FeOOH is facilitated (Ma *et al*., 2009).

3.2 Electrochemical impedance spectroscopy

Figures 4 and 5 show Nyquist diagrams of steels in saline solutions with contents of 3.5% m/v and 10% m/v NaCl. Table 2 shows the impedance results from an equivalent simulated circuit (Figure 6).

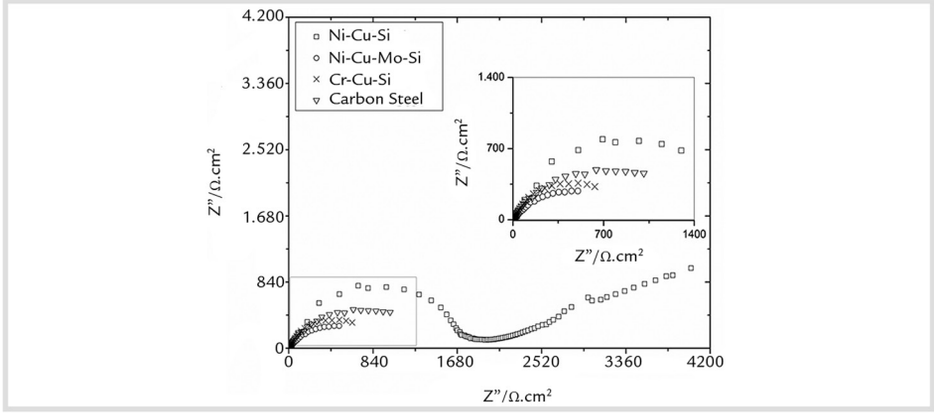

Figure 4
Nyquist diagrams of EIS data for different steels in 3.5% m/v NaCl.

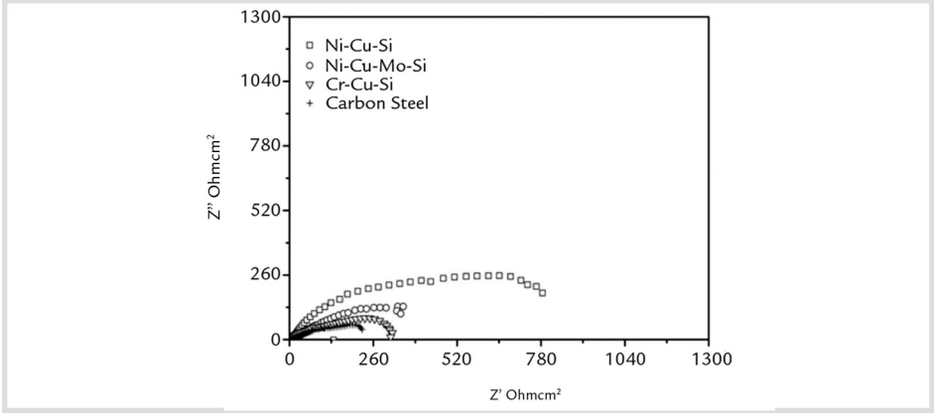

Figure 5
Nyquist diagram of steels in 10% m/v NaCl aqueous solution.

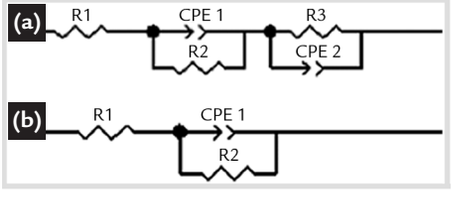

Figure 6
Equivalent circuits used to fit EIS data of (a) Ni-bearing and Cr-bearing steels in two electrolytes and carbon steel in 10% m/v NaCl solution and (b) carbon steel in 3.5% m/v NaCl solution.

For carbon steel, Cr-Cu-Si and Ni-Cu-Mo-Si alloyed steels in 3.5 % m/v NaCl solution, the EIS data were fitted using the equivalent circuit shown in Fig. 6 (a). A Randles circuit is an equivalent electrical circuit that consists of an active electrolyte resistance R_1 in series with the parallel combination of the double-layer capacitance Cdl which was replaced by a constant phase element (CPE_1) and an impedance of a faradaic reaction, R_2, which represents the charge transfer resistance (R_{ct}). The depressed semi-circles in the Nyquist diagram (Fig. 4 and Fig.5) can be explained by the heterogeneous nature of the solid surface or by the dispersion of some physical property values of the system (Belkaid *et al*., 2011). Conse-

quently, the layer at the interface cannot be considered as an ideal capacitor (n<1) and the constant phase element (CPE or Q) is often used as a substitute for the ideal capacitor (C).

For all of the other samples, the Nyquist diagrams (Fig. 4 and Fig. 5) can be represented by the electrical circuit $R_1(Q_1(R_2(Q_2R_3))$, that contains two-time constants. In this case, R_1 is the electrolyte resistance, while Q_1 (CPE_1) and R_2 are associated to the capacitance and impedance of the oxide layer. For the Ni-Cu-Si steels, the capacitive element associated to the oxide is related to a pure capacitor (C) and not to a constant phase element (CPE_1) since n is equal to one. The impedance at high frequency region corresponds to the resistance and capacitance of the oxide, consisting of a non-faradaic process (Li *et al*., 2010). The impedance of the oxide was the highest and the capacitance was the lowest for the Ni-Cu-Si steels, being the most protective layer among the steels studied, as shown in Table 2.

Li *et al* (2010) observed that the electrochemical reaction is observed at low frequencies of the Nyquist diagram. The capacitive arc at low frequency reflects the electrochemical process, accurately showing that the electric double layer and the charge transfer resistance as being a faradaic process. The electrochemical parameters Q_2 and R_3 are related to the double layer capacitance and impedance of a corrosive process occurring at the metal/corrosion product interface at low frequencies. The Ni-Cu-Si also showed the highest charge transfer resistance at the metal/corrosion product interface in a 3.5% m/v NaCl aqueous solution, being the most corrosion resistant in this saline medium. As the NaCl concentration increases, the impedance values decreased, except for the R_3 value of Ni-Cu-Mo-Si steel. in a 10% m/v NaCl solution, the charge transferring resistance (R_3) decreased for the Ni-Cu-Si and Cr-Cu-Si steels and remained unchanged for the Ni-Cu-Mo-Si steel which presented the highest value of R_3 and the highest impedance at the metal/corrosion product interface.

Table 2
Electrochemical parameters obtained using EIS analysis.

3.5% m/v NaCl	R_1 Ω.cm^2	Error (%)	CPE_1 F.s^n.cm^{-2}	Error (%)	R_2 Ω.cm^2	Error (%)	CPE_2 F.s^n.cm^{-2}	Error (%)	R_3 Ω.cm^2	Error (%)
SAE 1006	5.66	0.73	4.76 10^{-4}	1.14	1410	1.24				
Ni-Cu-Si	1.03	0.58	1.5510^{-10}	1.32	1722	1.60	3.9310^{-4}	1.99	3835	9.40
Cr-Cu-Si	5.83	0.67	1.0310^{-3}	1.25	975	1.59				
Ni-Cu-Mo-Si	4.32	0.27	1.3510^{-3}	0.53	907	0.59				
10% m/v NaCl										
SAE 1006	1.25	0.77	4.5810^{-3}	1.58	91	9.23	5.1410^{-5}	1.90	178	3.02
Ni-Cu-Si	1.70	0.70	2.0710^{-10}	1.61	799	8.38	5.0510^{-4}	2.38	100	1.70
Cr-Cu-Si	1.92	0.82	1.5510^{-3}	3.61	60	9.36	9.7410^{-3}	7.25	295	4.07
Ni-Cu-Mo-Si	2.73	0.50	2.1410^{-3}	4.30	29	6.47	7.3810^{-3}	1.78	504	1.88

Kihira *et al*. (1990) established a method for classifying the quality of rust based on electrochemical impedance measurements. According to these authors, typical impedance diagrams are characterized by a capacitive high-frequency arc whose real axis extrapolation is to provide rust resistance (RF) followed by another arc associated with the capacitive electric double layer parallel to the charge transfer resistance (R_{ct}), and finally a linear behavior associated with the Warburg impedance. In this study, a Warburg impedance was not observed. Based on field results, they claim that rusts with thickness less than 400 μm and R_{ct} exceeding 1 kΩ can be considered protective (Kihira *et al*., 1990). This criterion was also used by Wang *et al*. (1997). According to this criterion and data shown in Table 2, the rust that formed on the surface of Ni-Cu-Si was the most protective in the aqueous solution of 3.5% m/v NaCl.

The conductivity of 3.5% m/v NaCl solution is 76 S.cm^2 and 215 S.cm^2 for the 10% m/v NaCl content, and the values of electrolyte resistance of the 3.5% m/v NaCl solution were higher than those for the 10% m/v NaCl solution, as expected.

In both electrolytes, the rust layer of Ni-Cu-Si steel was the most protective, showing the lowest capacitance and the highest impedance. In the electrolytes of 3.5% m/v and 10% m/v NaCl aqueous solution, the Ni-Cu-Si steel showed the highest polarization resistance, as shown in Table 2.

The Ni-Cu-Mo-Si steel in a saline solution of 10% m/v NaCl showed a higher resistance than Cr-Cu-Si and the mild steel due to the highest charge transfer resistance at the metal/corrosion product interface. Thus, in a saline solution of 10% m/v NaCl, the most corrosion resistant steels were the Ni-bearing steels, in accordance with the results found by using field tests. It is important to emphasize that short-term experiments cannot give the same results as the long-term weathering tests because the oxide products must be quite different. The conditions of nucleation and mainly growth of corrosion products are different in an atmospheric field test and in an electrochemical test. However, the classification of the low alloyed steels considering the corrosion resistance using electrochemical tests in 10% m/v NaCl solution was similar to the rating that used field tests in a marine station. For the industry, the possibility of obtaining the classification of experimental steels in terms of the corrosion resistance by means of electrochemical tests of short duration is very relevant in the development of low alloyed steels. The results obtained herein represent an important tool for the research of low alloyed carbon steels. But it is clear that field tests are still necessary and useful for subsequent evaluation of the atmospheric corrosion resistance of steels.

4. Conclusions

The experimental Ni-Cu-Si and Ni-Cu-Mo-Si steels showed the lowest corrosion rates which decreased as the time increased after eight years of exposure in marine atmosphere. According to the electrochemical impedance spectroscopy in a saline solution of 10% m/v, the Ni-bearing carbon steels showed the highest corrosion resistance.

Lepidocrocite and goethite were identified in all oxidized steel surfaces after eight years of exposure in a marine atmosphere. Magnetite was detected in the oxide layer of Cr-Cu-Si and carbon steels. Akaganeite was identified only in the oxide layer of Ni-Cu-Si steels.

The classification of the low alloyed steels considering the corrosion resistance using electrochemical impedance spectroscopy in 10% m/v NaCl solution was similar to the rating when using field tests in a marine station, allowing to predict the classification of steels in terms of atmospheric corrosion resistance in a marine environment.

Acknowledgments

The authors are grateful to USIMINAS industry, Centro de Microscopia da UFMG, and Fundação de Amparo à Pesquisa do Estado de Minas Gerais (FAPEMIG). This study was funded by Conselho Nacional de Desenvolvimento Científico e Tecnológico, CNPq, (Grant number 303735/2015-5), and Coordenação de Aperfeiçoamento de Pessoal de Nível Superior, CAPES, (grant number 2011669426). The authors declare that they have no conflict of interest.

References

ALVARENGA, E. A., MOREIRA, J. G., BUONO, V. T. L. Influência da massa da camada de zinco na resistência à corrosão de aços eletrogalvanizados fosfatizados e pintados. In: CONGR. ANUAL ABM, 61, 2006. Rio de Janeiro. ***Anais...*** Rio de Janeiro: ABM, 2006.

BELKAID, S., LADJOUZI, M.A., HAMDANI, S. Effect of biofilm on naval steel corrosion in natural seawater. Journal of Solid State Electrochemistry, v.15, p. 525-537, 2011.

CHEN, Y.Y., TZENG, H.J., WEI, L.I., WANG, L.H., OUNG, J.C., SHIH, H.C. Corrosion resistance and mechanical properties of low-alloy steels under atmospheric conditions. Corrosion Science, v. 4, p. 1001–1021, 2005.

ITOU, M., TANABE, K., ITO, S., KUSUNOKI, T., USAMI, A., KIHIRA, H., TSUZUKI, T., TOMITA, Y. Performances of coastal weathering steel. ***Nippon Technical Report,*** n. 81, p. 79-84, 2000.

KAGE, I., MATSUI, K., KAWABATA, F. Minimum maintenance steel plates and their application technologies for bridge - life cycle cost reduction technologies with environmental safeguards for preserving social infrastructure assets. ***JFE Technical Report,*** n. 5, 2005.

KIHIRA, H., ITO, S., MURATA, T. The behavior of phosphorous during passivation of weathering steel by protective patina formation. ***Corrosion Science,*** v. 31, p.383-388, 1990.

KIMURA, M., KIHIRA, H., NOMURA, M., KITAJIMA, Y. Corrosion protection mechanism of the advanced weathering steel (Fe-3.0Ni-0.40Cu) in a coastal area. ***Electrochemical Society Proceeding,*** v. 14, p. 133-142, 2004.

LI, C., LI, Y., WANG, F. EIS monitoring study of atmospheric corrosion under variable relative humidity. ***Corrosion Science,*** v. 52, p. 3677-3686, 2010.

MA, Y.T., LI, Y., WANG, F. H. Corrosion of low carbon steel in atmospheric environments of different chloride content. ***Corrosion Science,*** v. 51, p. 997-1006, 2009.

McCAFERTY, E. ***Introduction to corrosion science.*** New York: Springer, 2010.

MORCILLO, M., DÍAZ, I., CHICO, B., CANO, H., DE LA FUENTE, D. Weathering steels: from empirical development to scientific design - a review. ***Corrosion Science,*** v. 83, p. 6-31, 2014.

NISHIMURA, T. Corrosion behavior of silicon-bearing steel in a wet/dry environment containing chloride ions. ***Materials Transactions,*** v. 48, p. 1438-1443, 2007.

SHIOTANI, K., TANIMOTO, W., MAEDA, C., KAWABATA, F., AMANO, K. Structural analysis of the rust layer on a bare weathering steel bridge exposed in a coastal industrial zone for 27 years. ***Corrosion Engineering,*** v. 49, p. 99-109, 2000.

TAKEMURA, M., FUJITA, S., MORITA, K., SATO, K., SAKAI, J. The protectiveness of rust on weathering steel in an atmosphere rich in airborne chloride

particles. ***Corrosion Engineering,*** v. 49, p.111-121, 2000.

TOSHIYASU, N. Corrosion behavior of silicon-bearing steel in a wet/dry environment containing chloride ions. ***MaterialsTransactions,*** v. 48, p.1438-1443, 2007.

WANG, Z., LIU, J., WU, L., HAN, R., SUN, Y. Study of the corrosion behavior ofweathering steels in atmospheric environments. ***Corrosion Science,*** v. 67, p. 1–10, 2013.

YAMASHITA, M., MIYUKI, H., MATSUDA, Y., NAGANO, H., MISAWA, T. The long-term growth of the protective rust layer formed on weathering steel by atmospheric corrosion during a quarter of a century. ***Corrosion Science,*** v. 36, p. 283-299, 1994.

YAMASHITA, H., MISAWA, T. Long-term phase change of rust layer on weathering steel with respect to Cr-substituted ultra-fine goethite. ***Corrosion Engineering,*** v. 49, p. 159-163, 2000.

YAMASHITA, M., ASAMI, K., ISHIKAWA, T., OHTSUKA, T., TAMURA, H., MISAWA, T. Characterization of Rust Layers on Weathering Steel Exposed to the Atmosphere for 17 years. ***Corrosion Engineering,*** v. 50, n.11, p. 521-530, 2001.

ZHANG, Q.C., WU, J.S., WANG, J.J., ZHENG, W.L., CHEN, J.G., Li, A.B. Corrosion behavior of weathering steel in marine atmosphere. ***Materials Chemistry and Physics,*** v. 77, p. 603-608, 2002.

Received: 23 November 2016 - Accepted: 25 April 2018.